



ELSEVIER

Journal of Luminescence 94–95 (2001) 805–809

JOURNAL OF  
LUMINESCENCE

www.elsevier.com/locate/jlumin

# Photon statistics in single-molecule fluorescence at room temperature

L. Fleury, J.-M. Segura, G. Zumofen\*, B. Hecht, U.P. Wild

*Physical Chemistry Laboratory, Swiss Federal Institute of Technology, ETH-Z, CH-8092 Zürich, Switzerland*

## Abstract

The fluorescence of single terrylene molecules in a crystalline host is investigated at room temperature by scanning confocal optical microscopy. Photon arrival times are analyzed in terms of inter-photon time distribution, second-order correlation function, and Mandel's  $Q$ -function. Nonclassical photon statistics is observed and a reverse intersystem crossing is detected that accelerates linearly with the applied laser power. Rate equations for the time evolution of the molecular level populations are shown to be appropriate for the analysis of the observations. © 2001 Elsevier Science B.V. All rights reserved.

*Keywords:* Photon statistics; Single-molecule spectroscopy; Scanning confocal optical microscopy

## 1. Introduction

Recent advances in fluorescence microscopy have rendered possible the detection, imaging and spectroscopy of single molecules (SMs) at various conditions [1–6]. Of particular interest here is the nonclassical photon statistics which is a signature for the quantum nature of the object under consideration. In the past, room temperature experiments that reveal the nonclassical character of SM fluorescence, could solely be performed by averaging the effects of a large number of single chromophores [7–9]. The reason for this is the limited amount of fluorescence photons available from a single molecule before photochemical destruction. Recently, it has been shown that for terrylene molecules embedded in a crystal of p-terphenyl the photochemistry is

drastically reduced so that a large number of photons could be recorded before photo bleaching [10,11]. Nonclassical photon statistics and an accelerated reverse intersystem crossing were observed and studied in terms of an appropriate system of rate equations for the level populations. The investigation of such and similar phenomena is essential for the development of an apparatus that generates single photons on demand [12–15]. In this paper we review our previous study and present more details about the data analysis.

## 2. Experimental

Crystal flakes of p-terphenyl with a thickness of  $\approx 3 \mu\text{m}$  doped with a low concentration of terrylene were grown by co-sublimation according to standard procedures [16]. A scanning confocal optical microscope was employed to image single molecules of terrylene in p-terphenyl [10].

\*Corresponding author. Fax: +41-1-632-1021.

E-mail address: zumofen@phys.chem.ethz.ch (G. Zumofen).

Terrylene was excited nonresonantly by a cw-Ar<sup>+</sup>-laser at a wavelength of 514 nm and a typical excitation intensity of 500 kW/cm<sup>2</sup>. The excitation light was focused to a diffraction-limited spot by an oil-immersion objective (Leica, 1.3 NA, ∞). The fluorescence light was collected by the same objective and directed to a 50/50 nonpolarizing beam splitter. The resulting two collimated fluorescence photon beams were focused in a Hanbury-Brown and Twiss arrangement onto two single-photon-counting avalanche photodiodes (SPAD). The output pulses of the two SPADs were then fed into separate inputs of a two-channel time interval analyzer (TIA).<sup>1</sup> An electronic delay was imposed on one channel in order to minimize the effect of noise generated by the TIA at very short inter-photon times. The dead time occurring in a single TIA channel is dominated by the dead time  $t_{\text{dead}} \approx 30$  ns of the SPAD. Photons arriving in different channels, however, can be recorded virtually free of dead time. In a typical experiment, the TIA acquires  $2 \times 10^6$  data points during  $\approx 20$  s indicating the arrival times with an accuracy of 0.5 ns as well as the acquisition channel for each detected photon. The molecules were, in general, stable enough to record data sets at several different excitation intensities before photo bleaching.

### 3. Analysis

A standard method of data analysis is based on the second-order correlation function [16–19]

$$g^{(2)}(\tau) = \langle I(t)I(t+\tau) \rangle / \bar{I}^2, \quad (1)$$

where  $I(t)$  is the photon detection rate at time  $t$  and  $\bar{I} = \langle I \rangle$ . Different experimental techniques have been applied to determine  $g^{(2)}$ . For short inter-photon times ( $< t_{\text{dead}}$ ) start–stop methods are widely used [20,5]. For larger times ( $> t_{\text{dead}}$ ), the evolution of the photon rate is usually recorded as a time trace from which  $g^{(2)}$  is calculated using an appropriate procedure [6,17].

In the present investigations we also examined independently the short and long time behavior of the autocorrelation function. The inter-photon

times were determined between a first photon recorded in one channel and the consecutive photon detected in the other channel. The corresponding histograms of the inter-photon times showed characteristic dips at the delay time  $t_{\text{delay}} \approx 48$  ns which were attributed to the photon antibunching [11]. For long times the arrival times of both channels were merged into bins of 0.5 μs length to generate time traces for  $I(t)$ . From these time traces the autocorrelation functions  $g^{(2)}(t)$  were calculated. As anticipated, photon bunching was detected indicating intersystem crossing. Surprisingly, the onset of photon bunching depended strongly on the laser power while the contrast was almost constant contrary to model predictions [11].

A more comprehensive analysis, that covers all time scales, is usually based on the renewal approach and on the two quantities  $K$  and  $J$  [11,19,21,22].  $K(t)$  is the probability density that the next photon is recorded at time  $t$  provided that there was a photon at  $t = 0$ .  $K$  is thus the distribution of inter-photon times.  $J(t)$  is the number density of photons at time  $t$  provided that there was a photon at  $t = 0$ . It is thus related to the second-order correlation function as  $J(t) = \bar{I}g^{(2)}(t)$ . According to the renewal approach  $J$  and  $K$  are related to each other by

$$J = K + K * K + K * K * K + \dots, \quad (2)$$

where  $*$  denotes convolution. In Laplace space this expression reads

$$\tilde{J} = \tilde{K} / (1 - \tilde{K}). \quad (3)$$

The situation is more complicated when the omnipresent background radiation is taken into account. In this case the recorded photon rate  $I(t)$  is the sum of the background radiation  $I_b(t)$  and SM fluorescence recorded rate  $I_m(t)$ , so that

$$I(t) = I_m(t) + I_b(t). \quad (4)$$

Correspondingly, we may distinguish between  $K$  and  $K_m$  for system and molecular inter-photon times, and similarly for the other quantities, e.g. for  $J$ ,  $g^{(2)}$ , and  $Q$ . Assuming a Poissonian process for the background radiation, one has [17]

$$\bar{I}J(t) = \bar{I}_m J_m(t) + 2\bar{I}_m \bar{I}_b + \bar{I}_b^2. \quad (5)$$

<sup>1</sup>Guide Technology, Sunnyvale, CA 94086, USA.

When combined, the independent Poissonian background and SM nonPoissonian radiation generate a photon stream which does not obey the renewal approach. Consequently, Eq. (2) does not apply in general while on the molecular basis

$$\tilde{J}_m = \tilde{K}_m / (1 - \tilde{K}_m) \quad (6)$$

is still valid. To see to which extent Eq. (3) breaks down we derived, similar to Eq. (5), a relationship between  $K$  and  $K_m$ , which reads

$$\bar{I}K(t) = \bar{I}_m(K_m + 2\bar{I}_b K_m^{(I)} + \bar{I}_b^2 K_m^{(II)})e^{-\bar{I}_b t}, \quad (7)$$

where

$$K_m^{(I)}(t) = \int_t^\infty K_m(t') dt',$$

$$K_m^{(II)}(t) = \int_t^\infty K_m^{(I)}(t') dt'. \quad (8)$$

As a result, there are two ways to relate  $K$  and  $J_m$  to each other, namely approximately based on Eqs. (3) and (5) and exactly using Eqs. (6) and (7). From model calculations we noticed that for a detection efficiency of  $\zeta \simeq 1$  and a relative background strength of  $\bar{I}_b/\bar{I}_m \simeq 1$  the relaxation rates obtained from the two methods may differ by  $\simeq 10\%$ . For the present study with  $\zeta$  less than 10% and background less than 20% we found that the deviations are less than 1%, well below the experimental accuracy, so that the more convenient method based on Eqs. (2) and (5) can be applied.

Accordingly, we calculated  $J$  numerically from the experimental histogram  $K$  of inter-photon times. This was done by replacing the Laplace transform in Eq. (3) by a fast Fourier transform. To avoid the problems with zero padding for functions which do not decay to zero at large  $t$  [23], we truncated the sum in Eq. (2) to a finite number  $N$  of terms. In general,  $N = 30\text{--}100$  lead to satisfactory results. Accounting further for the proper normalization of the  $J$  and  $K$  functions we could easily implement a procedure for the transformation. With this procedure we were able to calculate  $J$  from  $K$  over a time range of 6–7 orders of magnitude in a single run. An example is presented in Fig. 1. A pair of  $J$  and  $K$  functions are displayed according to the two ways of

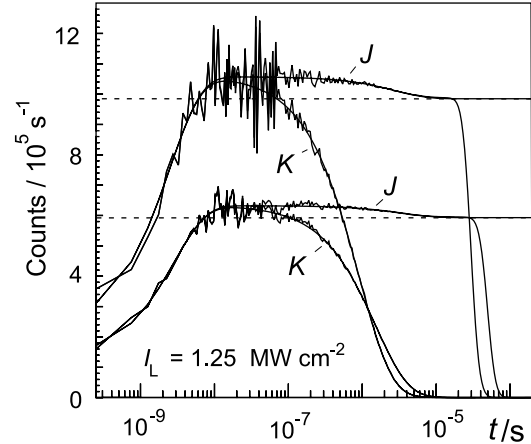


Fig. 1.  $K$  and  $J$  functions of molecule M1. The wiggly  $K$  functions are the normalized histograms obtained from the experimental inter-photon times determined in two ways: first photon from channel 1 and second from channel 2 and vice versa. The laser intensity was as indicated. The wiggly  $J$  functions were calculated using FFT. The smooth  $J$  and  $K$  functions are the predictions.

determining inter-photon times: first photon from channel 1 and second from channel 2 and vice versa. Because the detection efficiencies of the two recording channels were not identical there is a noticeable difference between the pairs of functions. Averages may be taken over the  $J$  but not over the  $K$  functions. As expected,  $J$  and  $K$  are indistinguishable for short times [21]. Deviations become apparent for times  $> 20$  ns. In particular, photon antibunching at short and photon bunching behavior at longer times are clearly visualized in a single plot [16]. We note the drop-off of the  $J$  functions at large  $t$  which results from the truncated series included in the method.

For further analysis of  $J$  and  $K$  we considered a system of rate equations which is appropriate at ambient conditions. The molecular levels  $S_0$ ,  $S_1$ , and  $T_1$  and the transition rates are shown schematically in Fig. 2. Here  $k_{12} = \sigma I_L$  denotes  $S_0\text{--}S_1$  pump rate depending on the cross-section  $\sigma$  and laser intensity  $I_L$ ,  $k_{21} = k_r + k_{nr}$  is the  $S_1\text{--}S_0$  relaxation rate with radiative and nonradiative component,  $k_{23}$  is the intersystem crossing rate, and  $k_{31}$  is the triplet relaxation rate. Considering the radiation from the  $S_1$  state, one has

Table 1  
Transition rates of molecules M1–M3<sup>a</sup>

Molecule	$\sigma$ ( $10^{-17}$ cm <sup>2</sup> )	$k_{21}$ ( $10^8$ s <sup>-1</sup> )	$k_{23}$ ( $10^5$ s <sup>-1</sup> )	$k_T$ ( $10^3$ s <sup>-1</sup> )	$k_{31}$ ( $10^4$ s <sup>-1</sup> )
M1	1.4	3.0	1.2	14.0	2–30
M2	7.5	1.2	23.0	3.5	2–30
M3	2.5	1.7	4.4	3.2	1–5

<sup>a</sup> Ranges of observed values are given for  $k_{31}$  (see footnote 2).  $k_T$  fixed for M2.

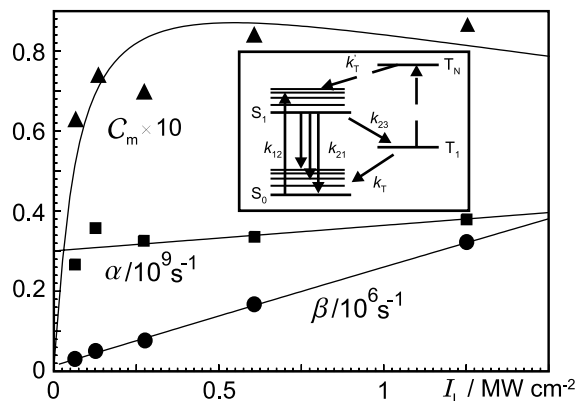


Fig. 2. Rates  $\alpha$  and  $\beta$  and contrast  $\mathcal{C}_m$  as a function of the excitation intensity  $I_L$ . Symbols denote the values obtained from fits to the experimental data of molecule M1. The full lines are the predictions. Inset: Scheme of relevant energy levels and transitions.

$J_m(t) = \zeta k_T \rho_{22}(t)$ ,  $\rho_{22}(0) = 0$ . The solution of the rate equations gives

$$J_m(t) = a(1 - e^{-\alpha t}) - b(1 - e^{-\beta t}). \quad (9)$$

Identifying  $\alpha$  and  $\beta$  with the fast and slow decay rates the first and second term relate to photon antibunching and bunching, respectively. The contrast resulting only from photon bunching is  $\mathcal{C}_m = b/(a - b)$ . For all molecules and for all laser intensities the variables  $\alpha$ ,  $\beta$  and  $\mathcal{C}_m$  were determined using Eqs. (5) and (9). Fitted  $J$  functions are shown in Fig. 1. From the adjusted parameters,  $K$  was calculated analytically using Eq. (3); the results are also shown in Fig. 1. The theoretical curves match the observations up to the experimental resolution.  $\alpha$ ,  $\beta$  and  $\mathcal{C}_m$  determined for several laser intensities are displayed in Fig. 2. From the rate equations  $\alpha$ ,  $\beta$  and  $\mathcal{C}_m$  are given in

terms of  $k_{12}, k_{21}, k_{23}, k_{31}$ . The analytical expressions are lengthy, for slow intersystem crossing approximate equations read:  $\alpha \approx \sigma I_L + k_{21}$ ,  $\beta \approx k_{31} + \sigma I_L k_{23} / (\sigma I_L + k_{21})$  and  $\mathcal{C}_m \approx \sigma I_L k_{23} / [k_{31}(\sigma I_L + k_{21})]$  [11].<sup>2</sup> Inserting the expression for  $\mathcal{C}_m$  in that of  $\beta$  one has  $\beta \approx k_{31}(1 + \mathcal{C}_m)$ . This expression is incompatible with the observations indicating, that  $\beta$  depends strongly on the laser intensity while  $\mathcal{C}_m$  is almost constant, unless a variation of  $k_{31}$  with the laser intensity is assumed. We therefore introduced the linear dependence  $k_{31} = k_T + k'_{31} I_L$  with  $k_T$  and  $k'_{31}$  as two independent parameters. With this assumption all results could be satisfactorily explained. The theoretical  $\alpha$ ,  $\beta$ , and  $\mathcal{C}_m$  are given in Fig. 2. The fitted parameters are collected in Table 1, the comparison with values of the literature is presented in Ref. [11]. We interpreted the dependence of  $k_{31}$  on the laser intensity as resulting from pumping higher triplet states [24], as shown in Fig. 2, resulting in an irreversible triplet relaxation rate. Interestingly, our data indicate that this effect may be one of the reasons for the remarkable photostability observed for terrylene in p-terphenyl because the molecules with a faster laser-induced triplet relaxation showed a weaker photo bleaching.

Photon antibunching and bunching is usually mentioned in the context of sub- and super-Poissonian statistics for photons detected in a given time interval. The occurrence of sub-Poissonian statistics is also a criterion of a nonclassical radiation field. For its characterization Mandel's  $Q$ -function, the normalized second

<sup>2</sup>Typing errors in Ref. [11] were brought to our attention by Dr. Hölzler. In the present paper we corrected for the range of  $k_T$  in Table 1 and for the approximate forms of  $\alpha$  and  $\beta$ .

factorial moment is considered,  $Q(T) = (\langle (\Delta n)^2 \rangle - \langle n \rangle) / \langle n \rangle$ , where  $n$  is the number of photons within a time interval  $T$  and  $(\Delta n)^2$  is the variance. Negative, zero, and positive  $Q$ -values indicate sub-, regular, and super-Poissonian behavior, respectively. The  $Q$ -function is related to  $J$  by [25]

$$Q(T) = \frac{2}{T} \int_0^T dt' \int_0^{t'} J(t'') dt'' - \bar{I}T. \quad (10)$$

For sufficiently short times,  $J$  can be approximated by  $K$ , so that  $Q(T)$  can be directly calculated from the recorded inter-photon time histogram. For terrylene in p-terphenyl a good agreement was achieved between prediction and experiment [11].

### Acknowledgements

We acknowledge stimulating discussions with H. Hölzler, A. Kramer, M. Kreiter, M. Prummer, A. Renn, B. Sick, R. Purchase, and W. Trabe-singer. This work was supported by the Swiss National Science Foundation and by the ETH-Zürich.

### References

- [1] W.E. Moerner, L. Kador, Phys. Rev. Lett. 62 (1989) 2535.
- [2] M. Orrit, J. Bernard, Phys. Rev. Lett. 65 (1990) 2716.
- [3] T. Plakhotnik, E.A. Donley, U.P. Wild, Annu. Rev. Phys. Chem. 48 (1997) 181.
- [4] W.E. Moerner, M. Orrit, Science 283 (1999) 1670.
- [5] T. Basché, W.E. Moerner, M. Orrit, H. Talon, Phys. Rev. Lett. 69 (1992) 1516.
- [6] X.S. Xie, J.K. Trautman, Annu. Rev. Phys. Chem. 49 (1998) 441.
- [7] F. De Martini, G. Di Giuseppe, M. Marrocco, Phys. Rev. Lett. 76 (1996) 900.
- [8] M. Wu, P.M. Goodwin, W.P. Ambrose, R.A. Keller, J. Phys. Chem. 100 (1996) 17406.
- [9] W.P. Ambrose, P.M. Goodwin, J. Enderlein, D.J. Semin, J.C. Martin, R.A. Keller, Chem. Phys. Lett. 269 (1997) 365.
- [10] L. Fleury, B. Sick, G. Zumofen, B. Hecht, U.P. Wild, Mol. Phys. 95 (1998) 1333.
- [11] L. Fleury, J.M. Segura, G. Zumofen, B. Hecht, U.P. Wild, Phys. Rev. Lett. 84 (2000) 1148.
- [12] B. Lounis, W.E. Moerner, Nature 407 (2000) 491.
- [13] C. Kurtsiefer, S. Mayer, P. Zarda, H. Weinfurt, Phys. Rev. Lett. 85 (2000) 290.
- [14] D.S. Englisch, E.J. Harbron, P.F. Barbara, J. Phys. Chem. A 104 (2000) 9058.
- [15] R.B. Brouri, A. Beveatos, J.-P. Poizat, P. Granger, Phys. Rev. A 62 (2000) 63 817.
- [16] S. Kummer, F. Kulzer, R. Kettner, T. Basché, C. Tietz, C. Glowatz, C. Kryschi, J. Chem. Phys. 107 (1997) 7673.
- [17] J. Bernard, L. Fleury, H. Talon, M. Orrit, J. Chem. Phys. 98 (1993) 850.
- [18] S. Kummer, S. Mais, T. Basché, J. Phys. Chem. 99 (1995) 17 078.
- [19] M.B. Plenio, P.L. Knight, Rev. Mod. Phys. 70 (1998) 101.
- [20] F. Diedrich, H. Walther, Phys. Rev. Lett. 58 (1987) 203.
- [21] S. Reynaud, Ann. Phys. (Paris) 8 (1983) 351.
- [22] P. Zoller, M. Marte, D.F. Walls, Phys. Rev. 35 (1987) 198.
- [23] W.H. Press, B.P. Flannery, S.S. Teukolsky, W.T. Vetterling, Numerical Recipes, Cambridge University Press, Cambridge, 1986.
- [24] C. Eggeling, J. Widengren, R. Rigler, C.A.M. Seidel, Anal. Chem. 70 (1998) 2651.
- [25] R. Short, L. Mandel, Phys. Rev. Lett. 51 (1983) 384.